

Mode interaction in horses, tea, and other nonlinear oscillators: The universal role of symmetry

Jacobus P. van der Weele^{a)}

Physics Department, University of Twente, P.O. Box 217, 7500 AE Enschede, The Netherlands

Erik J. Banning

Shell Oil, Bellaire Technology Centre, P.O. Box 481, Houston, Texas 77001

(Received 24 July 2000; accepted 15 March 2001)

This paper is about mode interaction in systems of coupled nonlinear oscillators. The main ideas are demonstrated by means of a model consisting of two coupled, parametrically driven pendulums. On the basis of this we also discuss mode interaction in the Faraday experiment (as observed by Ciliberto and Gollub) and in running animals. In all these systems the interaction between two modes is seen to take place via a third mode: This interaction mode is a common daughter, born by means of a symmetry breaking bifurcation, of the two interacting modes. Thus, not just any two modes can interact with each other, but only those that are linked (in the system's group-theoretical hierarchy) by a common daughter mode. This is the quintessence of mode interaction. In many cases of interest, the interaction mode is seen to undergo further bifurcations, and this can eventually lead to chaos. These stages correspond to lower and lower levels of symmetry, and the constraints imposed by group theory become less and less restrictive. Indeed, the precise sequence of events during these later stages is determined not so much by group-theoretical stipulations as by the accidental values of the nonlinear terms in the equations of motion. © 2001 American Association of

Physics Teachers.

[DOI: 10.1119/1.1378014]

I. INTRODUCTION

The world is full of coupled oscillators. One may think for instance of atoms in a crystal, vibrating around their lattice positions; or giant swarms of male fireflies flashing in perfect unison to attract females;¹ or even our own heart–lung system.² The physics of such systems is incredibly rich, and it is no wonder that they are the subject of much research. One of the problems of interest is *mode interaction*, i.e., the interaction between two or more basic modes of the system. During the last decade much insight has been gained into the way this interaction takes place, and that is what this paper is about.

If the oscillators (and the coupling between them) happen to be linear, everything is very simple: There is *no* interaction between the modes, because there are no mode-mixing terms in the Hamiltonian when written in terms of the normal modes. Any motion in the system is just a linear superposition of the normal modes. If the oscillators are nonlinear, however, the problem is much more complicated. In that case, the standard way to proceed is a frontal attack of the equations of motion. This gives detailed information about a particular system, but if one is interested in the general features of mode interaction, valid for all systems, a more conceptual viewpoint is required. The essence of the interaction, as we shall see, lies in the *symmetry* of the modes, and is best formulated in the language of group theory. This will be done in Sec. III.

Before we come to that, we first (in the present section) want to say something about the phenomenology of mode interaction, and in Sec. II we present a model system, consisting of only two pendulums and a spring. The group theoretical argument is given in Sec. III. In Sec. IV the validity of the argument is tested on a lively, seemingly far-fetched system (a galloping horse) and finally, in Sec. V, we make some concluding remarks.

Everyone who has ever put a cup of tea on a washing machine (vibrating, say, with a vertical amplitude a and frequency f) has performed the celebrated Faraday experiment, dating back as far as 1831.³ With a little luck one may have witnessed the formation of stable wave patterns on the fluid surface, and that is precisely the gist of the experiment. Two examples of such patterns, or modes, are sketched in Fig. 1. The modes oscillate at *half* the washing machine's frequency ($\frac{1}{2}f$) and are excited parametrically, in much the same way as the resonant oscillation of a parametric pendulum.

The parametric pendulum, depicted in Fig. 2(a), is a pendulum that is being moved up and down at its point of suspension.^{4–6} If the motion of this point is given by $z(t) = -a \cos \Omega t$, the equation of motion takes the form:

$$\ddot{\vartheta} + \gamma \dot{\vartheta} + \frac{1}{l}(g + a\Omega^2 \cos \Omega t) \sin \vartheta = 0. \quad (1)$$

This is the usual pendulum equation, $\ddot{\vartheta} + (g/l) \sin \vartheta = 0$, plus a few extra terms. The term $\gamma \dot{\vartheta}$ represents the unavoidable dissipation in the system (here taken to be a viscous damping in the point of suspension), and the driving is seen to manifest itself as a modulation of the gravitational acceleration g .

The downward equilibrium motion, or 0 motion, in which the pendulum simply goes up and down with the point of suspension, corresponds to a flat surface in the cup of tea; it is usually stable but *not* for combinations of a and Ω within the tongue-shaped regions in Fig. 2(b). (This is the well-known stability diagram of the damped Mathieu equation,⁷ to which Eq. (1) reduces if one sets $\sin \vartheta = \vartheta$, as usual for small perturbations from the downward equilibrium). Within these regions, small deviations from the 0 motion do not die out but are excited into an oscillatory motion. The main reso-

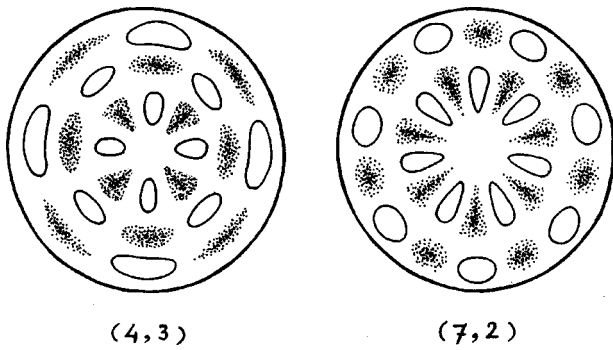


Fig. 1. Two surface patterns of the vibrating cup of tea (the Faraday experiment). Each pattern is characterized by two numbers, related to the number of maxima in the angular and radial directions, respectively.

nance occurs around $\Omega = 2\sqrt{g/l}$, i.e., at twice the natural frequency of the pendulum. As a consequence, the most important oscillations of the parametric pendulum (or of the tea surface) all have period $2T$, where T is the periodicity of the driving. Higher-order resonances are centered around the values $\Omega = (2/n)\sqrt{g/l}$, with $n=2,3,4,\dots$, but these are of much lesser importance.

So let us have a closer look at the main tongue. That is, let us follow a path through it as indicated in Fig. 3(a), adjusting the control parameters a and Ω in tiny steps, each time waiting until the pendulum has settled in its new steady motion.

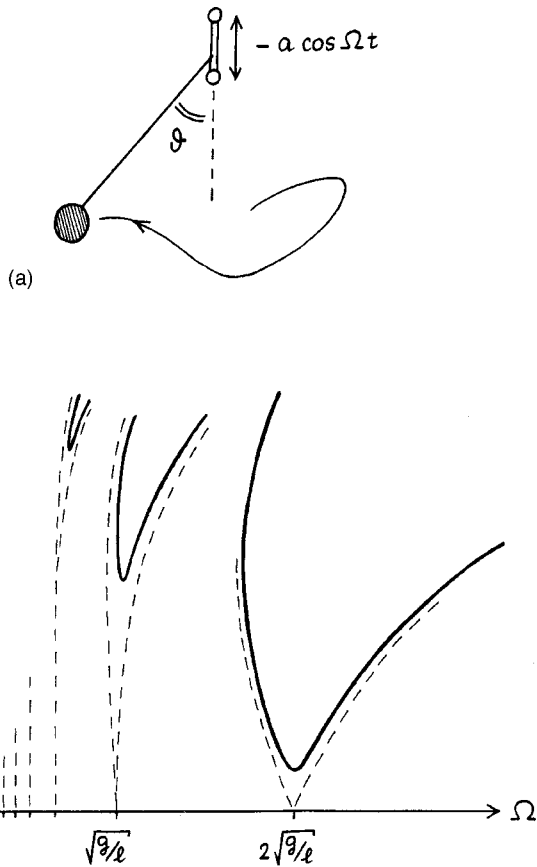


Fig. 2. (a) The parametric pendulum and (b) its stability diagram; the downward equilibrium is unstable for driving parameters a and Ω within the tongue-shaped regions. The dashed contours indicate the position of the regions of instability in the absence of dissipation.

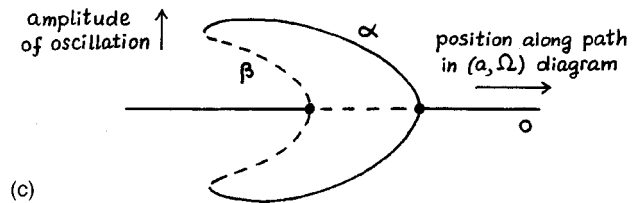
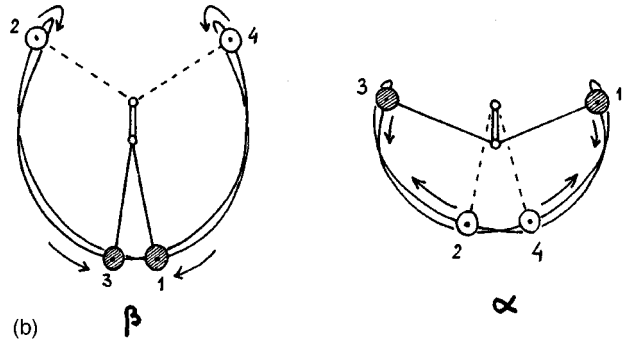
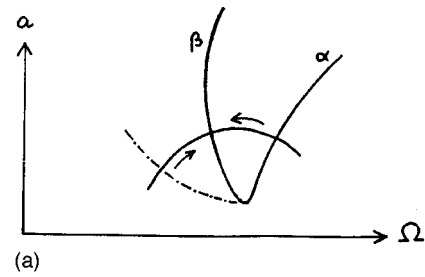


Fig. 3. (a) The path through the resonance tongue, (b) the α and β oscillations, and (c) the corresponding bifurcation diagram [i.e., amplitude of the various oscillatory motions vs position along the path in (a)]. The distinction between the α and β oscillations lies in their different phases with respect to the driving: The former reaches its amplitude shortly before the driving goes through its lowest position while the latter reaches its amplitude shortly after the driving goes through its highest position.

First we follow the path in the *counterclockwise* direction, i.e., from right to left. Outside the tongue the pendulum settles in the 0 motion, which is stable there, but as soon as we cross line α it undergoes a period doubling bifurcation⁸ and starts to perform the so-called α oscillation [sketched in Fig. 3(b)] with twice the driving period. Continuing our path through the (a, Ω) plane we find that, at line β , the 0 motion becomes stable again; this is the result of a second period doubling bifurcation, in which the unstable β oscillation of Fig. 3(b) is born. Now the pendulum has two stable motions to choose from (α and 0). If the experiment is performed gently enough, however, it will stay in the α oscillation. Following the path further, the α and β oscillations are seen to grow toward each other. At the dash-dotted line they meet and annihilate each other (a reverse saddle-node bifurcation⁸) and after that the pendulum has no other choice than to fall back to the 0 motion. The corresponding bifurcation diagram is given in Fig. 3(c). The bent curves are a clear reminder of the nonlinearity of the system: In a linear model—where the frequency of an oscillator, or a mode, does not depend on the amplitude—the lines α and β would go straight upwards, without ever meeting each other.

If we turn in our tracks and pursue the path in Fig. 3(a) in the *clockwise* direction, we witness a fine example of hysteresis, with a sudden jump from the 0 motion to a well-developed α oscillation upon crossing line β .

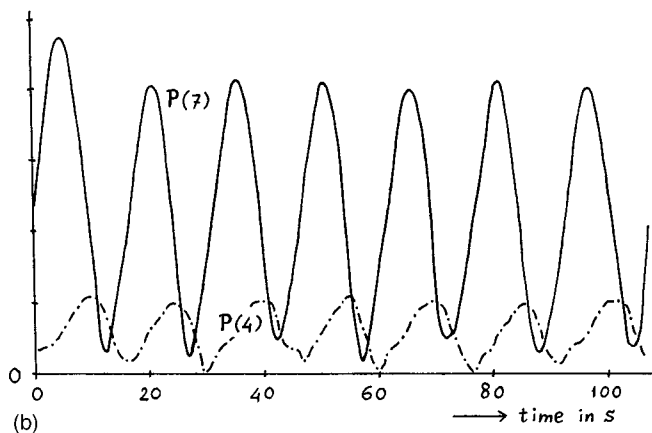
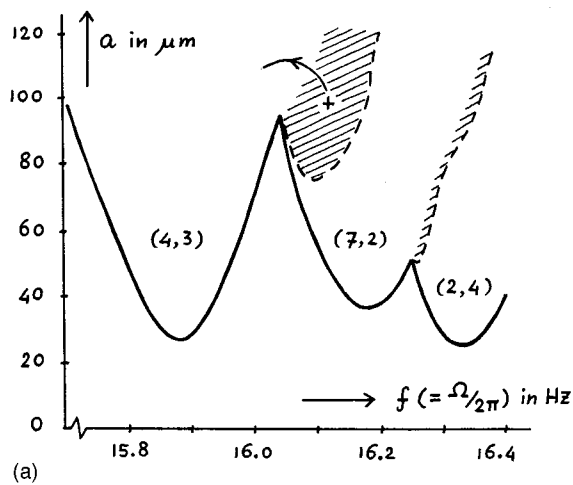


Fig. 4. (a) The (a, Ω) diagram of the Faraday experiment (after Ref. 9). We concentrate on the interaction between the (4,3) and (7,2) modes, but the diagram shows that similar interactions also occur between other pairs of modes. (b) The slowly varying heights of the peaks in the angular power spectrum associated with the sevenfold and the fourfold symmetries in the surface pattern, denoted as $P(7)$ and $P(4)$, after Ref. 9. The driving parameters are $a = 99 \mu\text{m}$ and $\Omega = 2\pi f = 101.3 \text{ rad/s}$, marked by the small cross in 4(a). If one follows the path indicated by the arrow, the signal undergoes a series of period doubling bifurcations, becomes chaotic, and eventually falls back upon the (4,3) mode.

The surface patterns in the Faraday experiment are created by the same kind of resonance.⁹⁻¹² When Ciliberto and Gollub⁹ performed the experiment in 1984 under precise laboratory conditions (with pure water instead of tea, and using the cone of a loudspeaker instead of a washing machine) they found a whole series of tongues, every one of them corresponding to a different mode. In Fig. 4(a) a small portion of the (a, Ω) plane is reproduced,⁹ showing the tongues that correspond to the modes of Fig. 1. Within the white regions labeled (4,3) and (7,2) they appear as individual modes, and in the intermediate hatched region they *interact*, giving rise to a wave pattern which contains characteristics of both the fourfold and the sevenfold mode (without, however, being a simple superposition of the two, since the superposition principle does not hold in a nonlinear system).

Figure 4(b), corresponding to the choice of parameters indicated by the small cross in Fig. 4(a), gives an impression of the interaction. The two curves represent the intensities $P(4)$ and $P(7)$, obtained by spatial Fourier analysis, of the four-

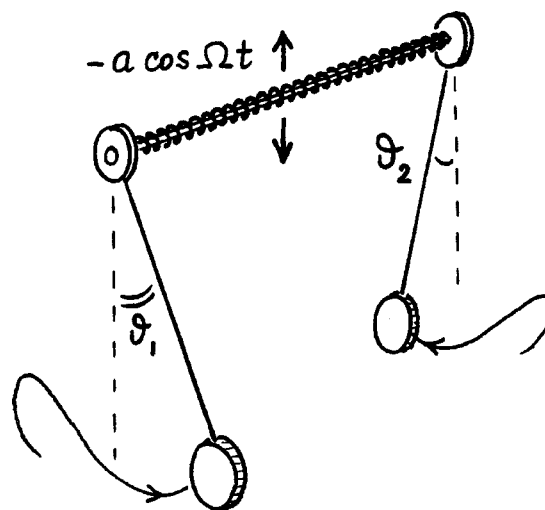


Fig. 5. A mechanical model to demonstrate mode interaction, consisting of two parametrically driven pendulums coupled by a torsion spring.

fold and the sevenfold components in the pattern; the signal oscillates with a periodicity of approximately 15 s, with $P(4)$ trailing one-quarter of a period behind $P(7)$. The motion is said to be quasiperiodic, since its period is incommensurate with the driving period (0.062 s). This is typical limit-cycle behavior and it means that the system has apparently gone through a Hopf bifurcation.⁸ Now, proceeding from the situation of Fig. 4(b), and carefully following the path indicated in Fig. 4(a), Ciliberto and Gollub found that the signal undergoes a period doubling bifurcation (after which its period is about 30 s), and a second one (bringing the period to 60 s), and soon thereafter becomes chaotic.⁹ Thus, in this case, mode competition leads to chaos, and that is exactly the title of their original paper. Eventually, if one proceeds further into the (4,3) tongue, the chaotic interaction breaks down and the fluid surface then “falls back” onto the pure (4,3) pattern. So the entire sequence is:

$$(7,2) \rightarrow \text{limit cycle} \rightarrow \text{period doublings} \rightarrow \text{chaos} \rightarrow (4,3).$$

This is all very beautiful, but also quite puzzling. First, why does the mode interaction take place within the territory of (7,2) and not, as might be expected, in the region where the two tongues overlap? Second, on a more technical level, how can a pure mode such as (7,2) undergo a Hopf bifurcation to a limit cycle? The answer to the latter question is that it cannot.^{12,13} That is, there must be an intermediate stage between the (7,2) mode and the limit-cycle interaction. (The later stages of the sequence, including the period doubling route to chaos, are all in good order).

To clarify these points it is not very convenient to stay with the cup of tea with its innumerable degrees of freedom and its notoriously hard-to-tackle Navier–Stokes equations (see, however, Refs. 10–12). Rather, we construct our own model, with just two degrees of freedom (the minimum number required) and relatively simple equations of motion. After all, it is not the tea we are interested in, but the general phenomenon of mode interaction.

II. THE TWO-PENDULUM MODEL

The mechanical system depicted in Fig. 5 is arguably the simplest model for studying nonlinear mode interaction.¹³⁻¹⁶ Indeed, it was especially devised for this purpose.¹⁴ It con-

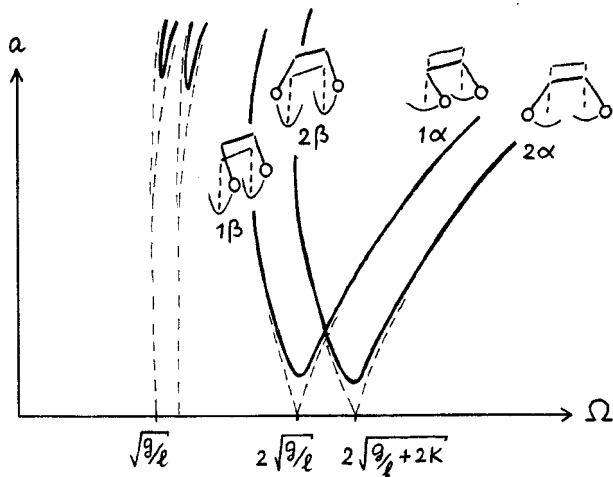


Fig. 6. The stability diagram for the 0 motion of the two-pendulum model. The 0 motion is unstable for driving parameters a and Ω within the tongue-shaped regions, and at the boundaries of these regions it gives birth (via a period doubling bifurcation) to the various oscillatory modes depicted.

sists of two identical pendulums coupled by a torsion spring, and is driven (parametrically) by the periodic up-and-down motion of the bar of suspension. The equations of motion are, including dissipation:¹⁵

$$\begin{aligned} \ddot{\vartheta}_1 + \gamma \dot{\vartheta}_1 + \frac{1}{l}(g + a\Omega^2 \cos \Omega t) \sin \vartheta_1 + f(\vartheta_1, \vartheta_2) &= 0, \\ \ddot{\vartheta}_2 + \gamma \dot{\vartheta}_2 + \frac{1}{l}(g + a\Omega^2 \cos \Omega t) \sin \vartheta_2 - f(\vartheta_1, \vartheta_2) &= 0. \end{aligned} \quad (2)$$

Here $f(\vartheta_1, \vartheta_2)$ is a function representing the coupling between the two pendulums. We take it to be slightly nonlinear (which is the most natural choice and, as it happens, also quite essential for our purposes):¹⁶

$$f(\vartheta_1, \vartheta_2) = K(\vartheta_1 - \vartheta_2) + L(\vartheta_1 - \vartheta_2)^3, \quad (3)$$

with L considerably smaller than K , say $K = 1.0 \text{ s}^{-2}$ and $L = 0.1 \text{ s}^{-2}$. The length of the pendulums (l) is chosen to be 1 m. In the present paper we consider only the dissipative case (with $\gamma \approx 0.1 \text{ s}^{-1}$) to make the link with practical applications such as the cup of tea as direct as possible. For the conservative case ($\gamma = 0$), which is also very worthwhile, we refer to Refs. 13–16.

The system has two basic oscillatory modes: one in which the pendulums swing in phase with each other and another one in which the pendulums move in counter-phase. The first one is very similar to the one-pendulum oscillation discussed in the previous section. In particular, it has the same eigenfrequency, since the (unstretched) spring does nothing to speed up or slow down the oscillation. The second mode has a somewhat higher eigenfrequency, because the motion is sped up by the torsion spring. Accordingly, each of the resonance tongues of the system is split into two as shown in Fig. 6. In the same figure we have sketched the various α and β oscillations which bifurcate from the 0 motion at the borders of the main double tongue.

As before, we follow a path through this double tongue [see Fig. 7(a)], slowly changing the parameters a and Ω , and we choose to go in the counterclockwise direction. We already know how the stability of the 0 motion changes along this journey. First it is stable (as indicated by a solid line in

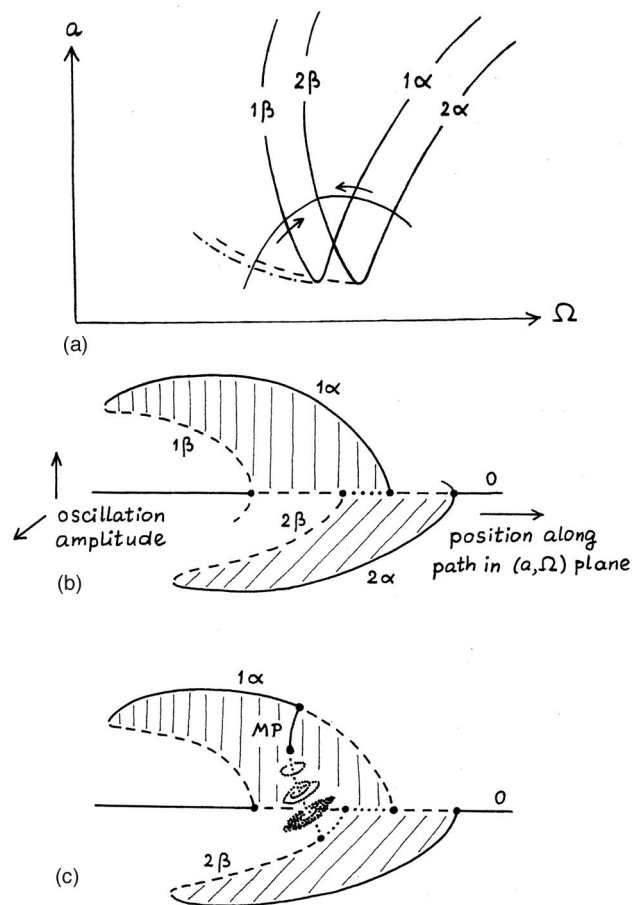


Fig. 7. (a) The path through the double resonance tongue, (b) the hypothetical (wrong!) bifurcation diagram obtained from applying the single-pendulum diagram twice, and (c) the true bifurcation diagram. The mode interaction is established by the cross branch (denoted by MP) connecting 1α and 2β . The circular loops around (the unstable part of) the MP branch represent a quasiperiodic oscillation, which undergoes a period-doubling bifurcation and eventually becomes chaotic.

the bifurcation diagram) and then, when we cross line 2α , it becomes unstable with respect to perturbations in the counter-phase direction while still retaining its stability in the in-phase direction (this semi-stability is indicated by a dashed line). Upon crossing 1α , it loses its stability in the in-phase direction as well, so here it becomes fully unstable (indicated by a dotted line). The stability in the counter-phase direction is regained at 2β (the line becomes dashed once more) and the stability in the in-phase direction at 1β (where the line becomes solid).

Now, one might be tempted to guess that the whole bifurcation diagram is just twice the old one-pendulum structure. If that were true, one would get the bifurcation diagram of Fig. 7(b). However, this diagram contains two bifurcational impossibilities:⁸ the 1α branch, at the point where it bifurcates from the 0 motion, should be semi-stable (dashed) and the 2β branch fully unstable (dotted). In the real bifurcation diagram [Fig. 7(c)] these shortcomings are cured by the cross branch denoted as MP. (MP stands for mixed phase, because in this mode the pendulums swing neither in phase nor in counter-phase; see Sec. III). Very conveniently, and in the same stroke, this cross branch establishes a link between the 1α and 2β modes, i.e., a *mode interaction*. With its Hopf bifurcation and subsequent period doublings, which lead to

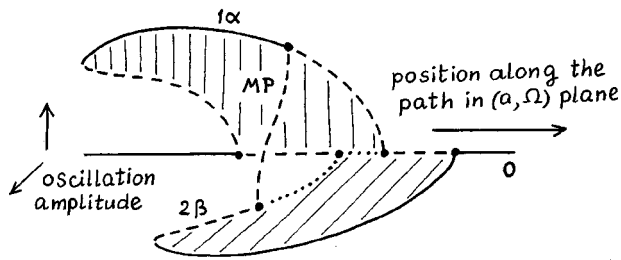


Fig. 8. The simplest scenario for mode interaction in the two-pendulum system, consisting of an unadorned cross branch. This is the scenario that occurs if the torsion spring between the two pendulums is chosen to be a soft one, i.e., if $L < 0$ in Eq. (3).

chaos, this interaction is obviously of the same type as that observed by Ciliberto and Gollub in the Faraday experiment. It is intrinsically nonlinear: The cross branch (let alone the transition to chaos) would not be present in a linear model.

The interaction scenario depicted in Fig. 7(c) is not the only one conceivable. Equally possible is the interaction depicted in Fig. 8, consisting of an unadorned cross branch, without any extra bifurcations, and no transition to chaos. In an experimental situation, this interaction would go by unnoticed, since the cross branch is unstable along its entire length.

Which scenario turns up in practice is determined by the nonlinear coupling term in the equations of motion.¹⁶ If the coupling is soft [i.e., if the coefficient L in Eq. (3) is negative] we get the simple scenario of Fig. 8, but a usual torsion spring is hard ($0 < L \ll K$) and then we get the more interesting scenario of Fig. 7(c).¹⁷ The point at which the bifurcation from 1α to MP occurs is insensitive to the value of L , because the stability of the 1α motion (in which the spring is not wound up) is not affected by the nonlinear coupling term. The bifurcation from the 2β branch, on the other hand, is extremely sensitive to the value of L . For increasing L the bifurcation point sweeps toward the right of the bifurcation diagram, and it is this circumstance that brings about the shift from one interaction scenario to the other.

Let us return to the path we were following through the (a, Ω) plane, around the intersection point of the tongues [see Fig. 7(a)], bearing in mind that for $L = 0.1 K$ we have to do with the scenario of Fig. 7(c). Now, what would we see of the interaction in an experimental situation, when only the stable motions count? The answer depends strongly on whether one goes in the clockwise or the counterclockwise direction.

The *counterclockwise* direction is rather uneventful: We first meet the stable 2α motion and (since we change the driving parameters very slowly, avoiding any unnecessary jumps) we *stay* with it along the whole length of the path. It simply does not become unstable.

In the *clockwise* direction, things are much more entertaining [see Fig. 9(a)]. Starting with the stable 1α motion we first witness, at the line denoted by MP, a symmetry breaking bifurcation to a stable MP mode. This MP mode subsequently becomes unstable by means of a Hopf bifurcation, which introduces an additional periodicity into the motion. In general, this periodicity is not a rational multiple of the period already present ($2T$), and the newly born motion will be *quasi-periodic*. In (stroboscopic) phase space such a motion takes the form of a limit cycle^{15,16} and that is why in Fig.

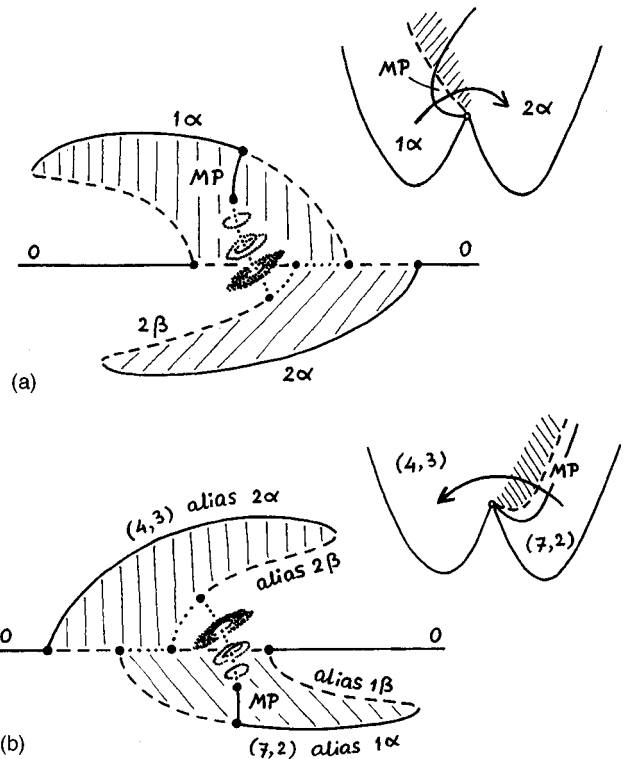


Fig. 9. (a) The bifurcation diagram, and the corresponding “experimental” sequence of events in the (a, Ω) plane, which one gets if one follows the path indicated (around the intersection point of the tongues), starting from the 1α mode. (b) The same for the Faraday experiment [starting from the $(7,2)$ mode, alias 2β]. In order to facilitate the comparison with the two-pendulum model we have indicated with which of the pendulum motions the various fluid patterns correspond. The shaded region in the (a, Ω) plane is the domain of mode interaction [including the regime of chaotic interaction, cf. Fig. 4(a)]. In the bifurcation diagrams, the circular loops around the unstable part of the MP branch correspond to a quasiperiodic interaction mode, which undergoes a period-doubling bifurcation and eventually becomes chaotic [cf. Fig. 7(c)].

9(a) it has been represented by a circular loop. This limit cycle subsequently undergoes a series of period doubling bifurcations and ends up as a chaotic attractor. When this attractor eventually loses its stability, the pendulums fall back to the first attracting motion that presents itself, which happens to be the 2α motion. So what we see in our experiment is the following sequence:

$$1\alpha \rightarrow \text{MP} \rightarrow \text{limit cycle} \rightarrow \text{period doublings} \rightarrow \text{chaos} \rightarrow 2\alpha.$$

This is summed up in Fig. 9(a), where the shading represents [as in Fig. 4(a)] the interaction region, including the chaotic regime. Note that the problem of the missing link between the pure mode and the limit cycle has been resolved: It is the MP mode. Actually, it is *this* mode that is at the heart of the whole interaction, and we will come back to it in Sec. III.

If we translate the above results to the Faraday experiment, we get the diagram of Fig. 9(b), which is clearly very similar to Fig. 9(a). There is only one difference worth mentioning, namely the orientation of the two pictures. Whereas in the two-pendulum system the pure modes are born toward the left, in the Faraday experiment they are born toward the right. This is because the pendulum modes happen to be *soft* ones, which means that their amplitudes grow in the direction of decreasing Ω ,¹⁶ whereas the corresponding fluid modes are *hard*, and grow in the opposite direction.^{11,12} As a

result, the complete bifurcation diagram, including the mode interaction (and the path one has to follow around the tongues' intersection point), has its direction reversed. That is why Ciliberto and Gollub had to go in the *counterclockwise* direction. In the clockwise direction they would have witnessed an abrupt transition from (4,3) to (7,2) without any intermediate mode interaction.

In closing the present section, we note that the question why the interaction region [i.e., the shaded region in the (a, Ω) plane] does not coincide with the overlap region of the tongues, has vanished into thin air. The overlap region is determined by the bifurcations of two pure modes (1α and 2β) from the 0 motion, whereas the interaction region is associated with the bifurcation of the MP motion from these pure modes. Only at the intersection point (where all these bifurcations happen to occur simultaneously) do the overlap region and the interaction region necessarily coincide.

III. SYMMETRY CONSIDERATIONS: THE NATURE OF THE INTERACTION MODE

A. The two-pendulum system

We have now come to the central section of the paper, in which it will be shown how the essence of mode interaction can be captured in terms of symmetry. We will do so both for the Faraday experiment and for the two-pendulum model, and we start with the latter, because it is the simpler of the two.

For our purposes, it is sufficient to consider the following three symmetries (in particular, we do not need to take into account the rotational symmetry of the pendulums).

1. Reflection (R)

This symmetry represents the fact that it does not make any difference for a (single) pendulum whether it swings toward the right or to the left. The corresponding transformation that leaves the equations of motion unchanged is:

$$\begin{matrix} R \\ (\vartheta_1, \dot{\vartheta}_1, \vartheta_2, \dot{\vartheta}_2, t) \rightarrow (-\vartheta_1, -\dot{\vartheta}_1, -\vartheta_2, -\dot{\vartheta}_2, t). \end{matrix} \quad (4)$$

2. Exchange (E)

This symmetry represents the fact that the two pendulums are identical and that it does not matter which one is called 1 and which is called 2. The corresponding transformation is simply an exchange of the indices:

$$\begin{matrix} E \\ (\vartheta_1, \dot{\vartheta}_1, \vartheta_2, \dot{\vartheta}_2, t) \rightarrow (\vartheta_2, \dot{\vartheta}_2, \vartheta_1, \dot{\vartheta}_1, t). \end{matrix} \quad (5)$$

3. Time translation (T)

The driving is periodic, so the equations of motion are unaltered by a time translation over one driving period $T = 2\pi/\Omega$. The corresponding transformation is:

$$\begin{matrix} T \\ (\vartheta_1, \dot{\vartheta}_1, \vartheta_2, \dot{\vartheta}_2, t) \rightarrow (\vartheta_1, \dot{\vartheta}_1, \vartheta_2, \dot{\vartheta}_2, t+T). \end{matrix} \quad (6)$$

The symmetry operations R and E are their own inverse, i.e., applying them twice yields the identity ($\mathbf{1}$). So in both cases, the operation plus the identity ($\{\mathbf{R}, \mathbf{1}\}$ and $\{\mathbf{E}, \mathbf{1}\}$, respectively) comprise a cyclic group consisting of two elements, commonly denoted as Z_2 .¹⁸ The third symmetry operation (T) also generates a Z_2 group if we restrict ourselves to

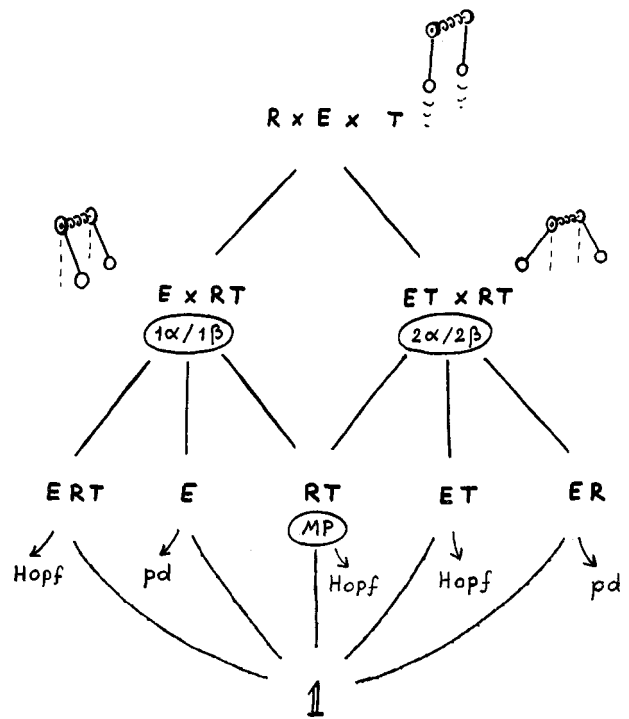


Fig. 10. The symmetry hierarchy (for $2T$ -periodic oscillations) of the two-pendulum system, in shorthand notation. The second level contains the basic modes. At the third level (which, among others, contains the interaction mode MP) it becomes possible to break away from the $2T$ periodicity, via either a period doubling (pd) or a Hopf bifurcation.

periodic motions of period $2T$ (and identify $t=0$ with $t = 2T$); in the present context this can hardly be called a restriction since all the oscillations taking part in the mode interaction have period $2T$. The three operations R , E , and T may be applied to the system (i.e., the equations of motion) independently of each other, and in any desired order, so we arrive at the symmetry group $Z_2(\mathbf{R}) \times Z_2(\mathbf{E}) \times Z_2(\mathbf{T})$.

The only motion that is invariant under all three operations is the 0 motion, and to a group theorist this motion must certainly be the most perfect and beautiful of all. (The 0 motion is even more symmetrical than suggested here, since we deliberately regard it as having periodicity $2T$, while it actually repeats itself after every driving period T : the pendulums simply go up and down with the bar of suspension). The other motions are all less symmetrical. For instance, the 1α oscillation is invariant under the exchange transformation E and the combined operation RT , but not under R or T independently. It thus has symmetry group $Z_2(\mathbf{E}) \times Z_2(\mathbf{RT})$, which is a subgroup of the original $Z_2 \times Z_2 \times Z_2$ group.¹⁸ Likewise, each oscillation of period $2T$ falls in one or the other subgroup, which together form the so-called isotropy lattice depicted in Fig. 10. The perfect symmetry of the 0 motion (at the top of the hierarchy) can be broken step by step, by means of symmetry breaking bifurcations, until one reaches the bottom of the lattice. The oscillations at this lowest level have none of the above symmetries anymore.

The first step brings the 0 motion to one of the "pure" modes: that is, either to $Z_2(\mathbf{RT}) \times Z_2(\mathbf{E})$, corresponding to 1α and 1β , or to $Z_2(\mathbf{RT}) \times Z_2(\mathbf{ET})$, corresponding to 2α and 2β . (Of course, the α and β versions of the modes belong to the same symmetry class, otherwise they would never be

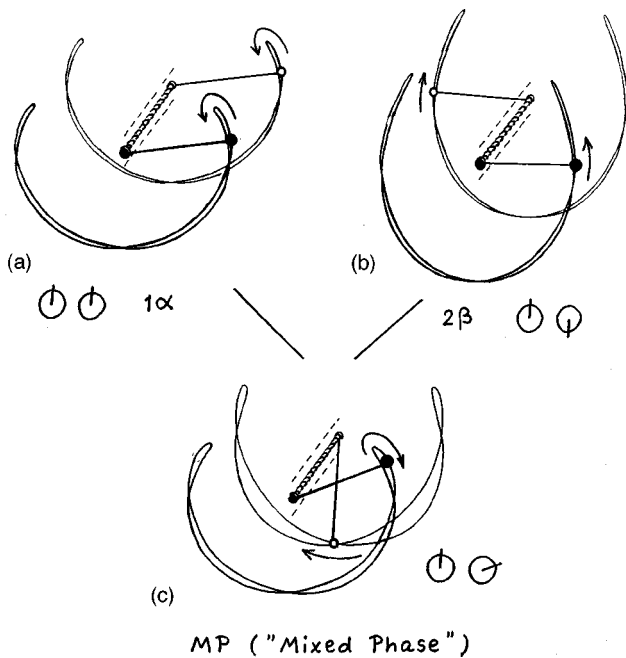


Fig. 11. The main actors in the mode interaction: (a) the 1α motion, (b) the 2β motion, and (c) their common daughter, the MP motion. Also shown are the corresponding phase pictograms, i.e., the “clocks” that indicate the phase difference between the two pendulums.

able to annihilate each other). These pure modes are still quite symmetrical. Too symmetrical in fact to admit any escape from the lattice (to motions beyond period $2T$) by either a period doubling or a Hopf bifurcation:¹³ They *have* to undergo a symmetry breaking bifurcation, bringing us to the third level in the lattice. It is at this level that Hopf bifurcations [for the oscillations with $Z_2(\mathbf{E}\mathbf{T})$, $Z_2(\mathbf{R}\mathbf{T})$ or $Z_2(\mathbf{R}\mathbf{E}\mathbf{T})$ symmetry] or period doublings [for those with $Z_2(\mathbf{R}\mathbf{E})$ or $Z_2(\mathbf{E})$ symmetry] and the associated routes to chaos can come into play.^{13–16} It is also at this level that the mode interaction takes place: The pure modes have a common daughter, with $Z_2(\mathbf{R}\mathbf{T})$ symmetry, and it is through *her* that they interact.

Mode interaction is conceivable between any two pure modes in Fig. 10 (as, in fact, between any two modes that share a daughter in the hierarchy) but only the interaction between the 1α and 2β modes has actually been observed. This has to do with the fact that this pair is “anchored” (to the 0 motion) at the intersection point of the two tongues, which serves as a nucleation point for the mode interaction. The other pairs lack such a nucleation point. In more technical terms, it is called a critical point of codimension 2, meaning that two linear instabilities occur simultaneously. Indeed, the connection between the existence of such a point and the appearance of mode interaction is so direct that some authors¹² simply identify the two, calling any point of this kind a “mode interaction point.”

In Fig. 11, which is an enlargement of the crucial part of the symmetry lattice, we have drawn the 1α and 2β modes together with their common daughter. The latter has been given a name already in Fig. 7(c), namely MP, which stands for mixed phase; this is because it possesses neither \mathbf{E} nor $\mathbf{R}\mathbf{E}$ symmetry, i.e., the pendulums swing neither in phase nor in counter-phase but in a kind of *mixed* phase. A good way to

represent the phase relations between the pendulums is by means of so-called phase pictograms, i.e., the little “clocks” in Fig. 11. The arm of each clock makes one revolution per $2T$ seconds. In the 1α mode the arms move in phase with each other, in the 2β mode they move in exact counter-phase, and in the MP motion they have some intermediate phase difference.

It is tempting to interpret the MP motion as a superposition of 1α and 2β , but this is in fact a misrepresentation for at least three reasons. First, the superposition principle does not hold in a nonlinear system. Second, it would suggest that the MP motion can be stable only when (both) its parents are stable, but this is in plain contradiction with the facts. Third, the MP motion is separated by a bifurcation from its parents, so it really is a mode in its own right. In this context it is perhaps good to note that the nonlinear nature of the interaction, which shows up so clearly in the bifurcation diagram, is of no concern to the symmetry lattice. The lattice does not discriminate between linear and nonlinear systems, as long as they have the same overall symmetry. But the fact is that a nonlinear system makes much more creative use of the possibilities offered by the lattice. [In particular, if the system were linear the $\mathbf{R}\mathbf{T}$ subgroup would indeed stand for nothing more than a simple superposition (not an interaction) of the two pure modes.]

B. Faraday’s cup of tea

How does all this work out for the cup of tea? Well, to begin with, the symmetry structure of the Faraday experiment differs somewhat from that of the two-pendulum model (which is rather fortunate, since it makes it easier to see which parts of our discussion are generally valid and which are not). The time-translation symmetry $Z_2(\mathbf{T})$ is the same, but the spatial symmetries $Z_2(\mathbf{R}) \times Z_2(\mathbf{E})$ are replaced by $O(2)$, the orthogonal group in two dimensions, which says that the (circular) surface of the fluid is invariant under all continuous rotations around the center, and all mirror reflections in axes that pass through the center.¹⁸ The subgroups of $O(2) \times Z_2(\mathbf{T})$ that correspond to the (4,3) and (7,2) modes have been sorted out by Crawford, Knobloch, and Riecke¹² and turn out to be $D(\mathbf{M}, (2\pi/8)\mathbf{T})$ and $D(\mathbf{M}, (2\pi/14)\mathbf{T})$. Here $D(\mathbf{M}, (2\pi/k)\mathbf{T})$ is a dihedral group generated by \mathbf{M} , which is a mirror reflection in a properly chosen axis, and the element $(2\pi/k)\mathbf{T}$, which represents a rotation over $2\pi/k$ rad combined with time translation over one driving period. The symmetry of the pure modes does not allow them to undergo a Hopf bifurcation^{12,13} so there can be no question of a time-varying interaction [as in Fig. 4(b)] before they have undergone a symmetry breaking, bringing us to the third level of the isotropy lattice in Fig. 12. Here we see something new: The modes (4,3) and (7,2) have *two* common daughters and can interact via any one of them. The daughters are fairly alike; their symmetry groups indicate that the “properly chosen” axis of reflection remains fixed in both cases, implying that the associated wave patterns have no azimuthal drift. Both modes can undergo a Hopf bifurcation (which preserves the Z_2 symmetry) and thus give birth to the more complicated interaction form of Fig. 4(b).^{8,12} The only difference between them is that one [$Z_2(\mathbf{M})$] is invariant under mirror reflection, and the other one [$Z_2(\mathbf{M}\mathbf{T})$] is invariant under the *combined* operation of mirror reflection

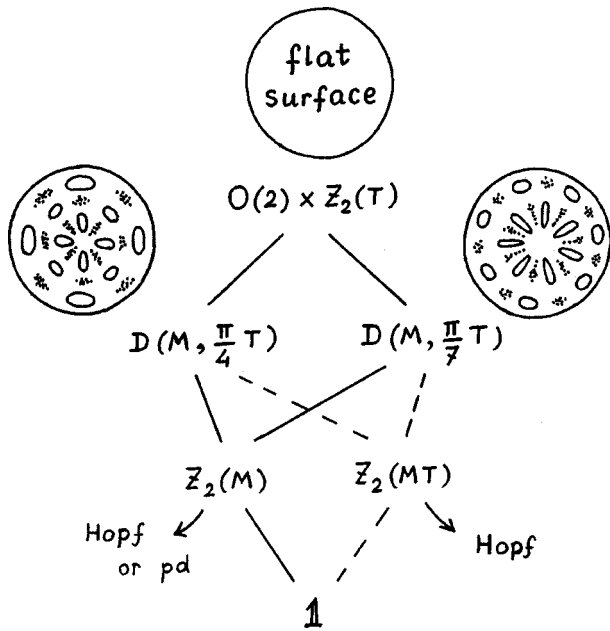


Fig. 12. The symmetry hierarchy for the (4,3)–(7,2) mode interaction in the Faraday experiment (after Ref. 12). As in Fig. 10, we have also indicated the escape routes from the lattice, via period doubling (pd) and Hopf bifurcations.

and time translation. Ciliberto and Gollub did not specify whether they were dealing with $Z_2(\mathbf{M})$ or $Z_2(\mathbf{MT})$ symmetry, but they *did* mention that the interaction patterns had no azimuthal drift.

What is more surprising, at least at first sight, is that they observed neither of the two daughters at all (the third level of the lattice in Fig. 12), whereas these *should* have come between the (7,2) mode and the quasi-periodic interaction of Fig. 4(b). One explanation may be that the associated zone in the (a, Ω) plane is quite narrow, which means that the interaction mode in this zone is still almost indistinguishable from the (7,2) mode (even more so because they have the same periodicity $2T$). The explanation may also be sought in slight imperfections in the symmetry of the experimental setup. These would cause an unfolding of the symmetry breaking bifurcation, turning the transition from the pure mode to the interaction mode into a gradual one. In that case it becomes meaningless to distinguish between the two: They would belong to the same symmetry class, and would form an uninterrupted branch in the bifurcation diagram. If the symmetries are intact, however, the $2T$ -periodic interaction zone (however small) must be there.

In any case, the general rule for nonlinear mode interaction is that two modes interact via a common daughter mode. It is this rule that makes the mode interaction in the two-pendulum system [Fig. 9(a)] so similar to that in the Faraday experiment [Fig. 9(b)]. Thus, as anticipated in the introduction, the results of Ciliberto and Gollub can be understood (and even supplemented) by means of the two-pendulum model.

We could stop here, but that would be a pity. Until now we have been talking about only two systems, but the “general rule” formulated above would hardly deserve that name if it would not apply to a multitude of other systems too. Let us therefore discuss an example of mode interaction that comes from an entirely different field: animal gaits.



Fig. 13. A trotting horse, as photographed by Muybridge (from Ref. 19).

IV. ANIMAL GAITS

The legs of animals are among the finest coupled oscillators to be found in nature, and the oscillation patterns (or “gaits”) used in locomotion are singularly fascinating.^{19–29} It does not matter whether the animal has two legs (ostrich), four (horse), six (ant), eight (spider) or more (centipede), each has its own charm. Also the more unusual cases with an odd number of legs are very interesting; in Ref. 22 a three-legged dog is discussed, and in Ref. 25 a man with a walking stick. Fortunately for us, N -legged locomotion can be described quite adequately by N parametrically driven pendulums. For instance, two-legged locomotion (if one is willing to disregard the effects of arms, tails, etc.) is described by our two-pendulum model: Humans normally use a 2 mode, whereas a jumping kangaroo uses a 1 mode.

Things get more interesting with four legs. The paragon of quadrupeds is undoubtedly the horse, which is able to perform an amazing variety of gaits: walk, trot, gallop, canter, to name just a few. Modern gait analysis began with the trot. The story goes²² that in the 1870s two rich Americans, Stanford and McCrellish, had a bet (for no less than \$25,000) over the placement of the feet of a trotting horse. Stanford asserted that there were moments when the horse had all of its feet off the ground, and McCrellish disputed this. Now, it is virtually impossible to settle this question with the naked eye, so they called in the help of a photographer named Muybridge, who invented the “zoopraxiscope” (a series of interconnected cameras) to produce the first movie of a trotting horse. Figure 13 shows four pictures from this movie, which—understandably—delighted Stanford more than McCrellish.³⁰

Our model of a horse, or more generally of any four-legged animal, is shown in Fig. 14. It is a natural extension of our two-pendulum model, consisting of four pendulums coupled by various springs. Experienced gait analysts will notice that it is closely related to the “type 2” quadruped of Refs. 22 and 23. The major difference is that we have added an explicit, parametric driving. (The authors of Refs. 22 and 23 did not use pendulums but limit-cycle oscillators of the Van der Pol type, which means that the periodicity in their system was introduced by means of a Hopf bifurcation). The driving represents the signal from the brain (or perhaps some other part of the nervous system) that tells the animal to run and, since it is parametric, the principal gaits it produces will have twice the driving period. The model is something of a caricature, to be sure, but the results turn out to be remarkably realistic.

The corresponding equations of motion are:

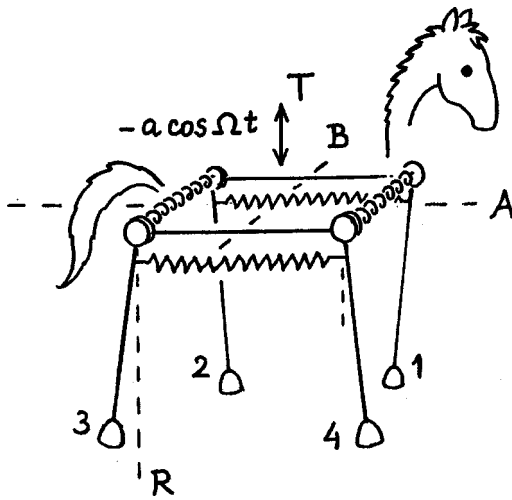


Fig. 14. Our model of a four-legged animal. We have indicated the four symmetry operations of this (idealized) system: **A** is the left–right exchange, **B** the front–hind exchange, **R** denotes reflection of the pendulums, and **T** is time translation over one driving period. The head and tail are supposed to be massless.

$$\begin{aligned}
 \ddot{\vartheta}_1 + \gamma \dot{\vartheta}_1 + \frac{1}{l}(g + a\Omega^2 \cos \Omega t) \sin \vartheta_1 + f_B(\vartheta_1, \vartheta_2) \\
 + f_A(\vartheta_1, \vartheta_4) = 0, \\
 \ddot{\vartheta}_2 + \gamma \dot{\vartheta}_2 + \frac{1}{l}(g + a\Omega^2 \cos \Omega t) \sin \vartheta_2 + f_B(\vartheta_2, \vartheta_1) \\
 + f_A(\vartheta_2, \vartheta_3) = 0, \\
 \ddot{\vartheta}_3 + \gamma \dot{\vartheta}_3 + \frac{1}{l}(g + a\Omega^2 \cos \Omega t) \sin \vartheta_3 + f_B(\vartheta_3, \vartheta_4) \\
 + f_A(\vartheta_3, \vartheta_2) = 0, \\
 \ddot{\vartheta}_4 + \gamma \dot{\vartheta}_4 + \frac{1}{l}(g + a\Omega^2 \cos \Omega t) \sin \vartheta_4 + f_B(\vartheta_4, \vartheta_3) \\
 + f_A(\vartheta_4, \vartheta_1) = 0.
 \end{aligned}
 \tag{7}$$

The numbering of the legs is as in Fig. 14, and the indices *A* and *B* indicate that the cross-wise springs are different from the springs along the sides of the animal. This set of equations may look somewhat forbidding, but one thing at least is clear: Just like any system of four coupled oscillators, our model has four basic modes. And these modes are associated with four tongues of resonance in the (a, Ω) plane, as shown in Fig. 15, where we have also included the corresponding phase pictograms.

The first, slowest basic mode is the one in which all the pendulums move in phase with each other, as if they were one single object (the springs are inactive). The angular eigenfrequency of this mode is precisely the same as that of one single pendulum (namely $\sqrt{g/l}$), which means that the tongue originates at $\Omega = 2\sqrt{g/l}$. In the second and third tongues half of the springs (two out of four) are active. The front–hind version originates at $\Omega = 2\sqrt{g/l + 2K_B}$, and the left–right version at $\Omega = 2\sqrt{g/l + 2K_A}$, so the order of these two depends on the relative strength of K_A and K_B . In Fig. 15 we have taken the cross-springs (*A*) to be somewhat stronger than the longitudinal (*B*) springs, but (depending on the

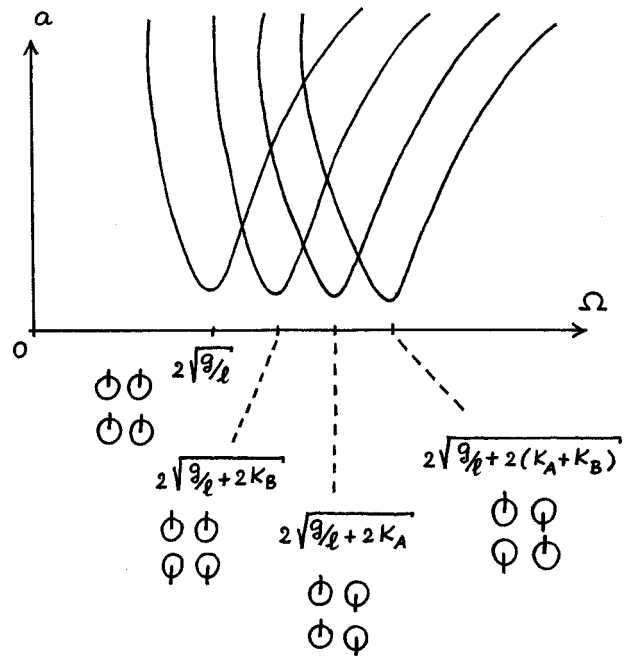


Fig. 15. The four basic modes of the four-pendulum model in Fig. 14, and their corresponding resonance tongues in the (a, Ω) plane. Also included are the corresponding phase pictograms.

animal) this might also be the other way around. The fourth basic mode, at $\Omega = 2\sqrt{g/l + 2K_A + 2K_B}$, is the fastest one, with all four springs in action.

In real life these four basic modes are known as the prong, the bound, the pace, and the trot. The prong [see Fig. 16(a)] is a relatively rare gait, in which the animal propels itself

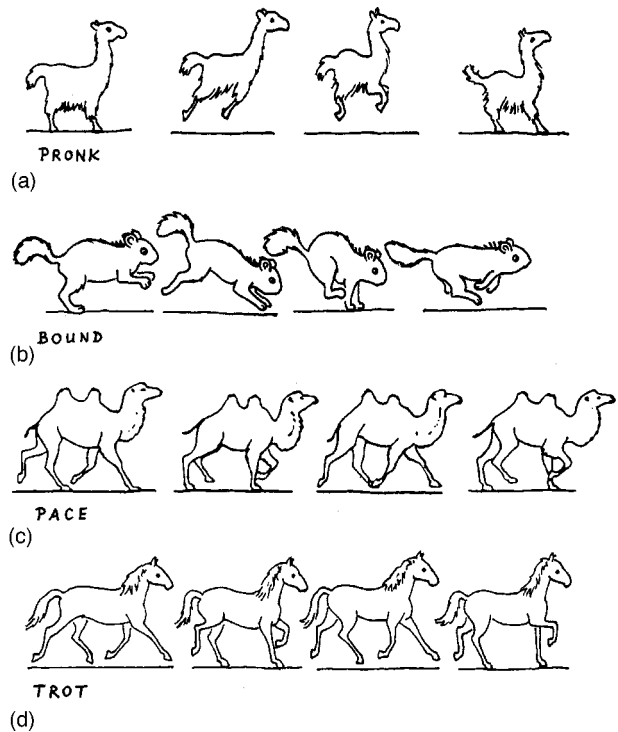


Fig. 16. The four basic gaits, corresponding to the basic modes of our four-pendulum model: (a) prong, (b) bound, (c) pace (or rack), and (d) trot. The pictures of the latter three are adapted from Ref. 19.

stiff-leggedly through the air. It is used by startled deer and antelopes, by playful kittens, and occasionally also by llamas, especially around dusk. Whole groups of llamas have been seen to prong back and forth across a field, or in a circle, to play or to ward off predators.²⁷

The second basic mode is called the bound, see Fig. 16(b). Aristotle (in an early standard work on animal gaits, around 350 B.C.) called this “a kind of stumbling forwards.” He thought it would be hard to maintain, as indeed it is for larger animals, but for a number of small mammals (like the ground squirrel depicted here) the bound is in fact the usual fast gait.

The third basic mode [Fig. 16(c)] goes by the name of pace, or rack. Also considered unsatisfactory by Aristotle (since the weight must be shifted all the time, following the side of support), this is nevertheless the typical gait of camels. Other animals to which the pace comes naturally are canines (dogs, coyotes) and Icelandic horses. Most other horses have to be trained to do it, sometimes with a harness around their legs.

The fourth basic mode is the trot [Fig. 16(d)]. This is the gait we met before, which race horses are able to maintain up to admirable speeds. Sometimes, however, they “break into a gallop”. The trot is also the gait by which dogs are judged in the show ring.

To find out how these pure modes interact, and how our quadruped can switch from the one to the other, we exploit again the symmetries (and, more specifically, the group theoretical structure) of the system. This is a relatively new idea in gait analysis^{21–26} and has already proved to be very fruitful. In the present model there are *two* exchange symmetries: The exchange between left and right legs (**A**) and the exchange between front and hind legs (**B**). The first symmetry is fairly perfect in most animals, but the second one is of course only approximate (a head is not a tail, after all). Then there is the reflection symmetry **R** of the pendulums. The average animal leg is admittedly less symmetric than a pendulum, but some internal symmetry may nevertheless be present, and this is represented by **R**. And finally, of course, we have the time-translation symmetry **T**.

Once one has identified the symmetries of the system, it is not difficult to construct the symmetry hierarchy. This is done in Fig. 17. The most symmetrical gait of all is the 0 motion, corresponding to the full symmetry group $Z_2(\mathbf{A}) \times Z_2(\mathbf{B}) \times Z_2(\mathbf{R}) \times Z_2(\mathbf{T})$, or $\mathbf{A} \times \mathbf{B} \times \mathbf{R} \times \mathbf{T}$ for short. This might be called the “hop.” The animal goes up and down, but not forward, and for this reason it is not useful for locomotion. Impatient bulls before the start of a rodeo do something of the kind, but our interest lies not with the hop. We immediately go on to the four modes that can be derived from it, i.e., the ones that correspond with the four resonance tongues in the (a, Ω) plane. These are of course just the basic modes, which are described by the subgroups $\mathbf{A} \times \mathbf{B} \times \mathbf{RT}$, $\mathbf{A} \times \mathbf{BT} \times \mathbf{RT}$, $\mathbf{AT} \times \mathbf{B} \times \mathbf{RT}$, and $\mathbf{AT} \times \mathbf{BT} \times \mathbf{RT}$, respectively. In the latter three the legs are pairwise in phase, and the two in-phase pairs move in exact counter-phase with each other, as exemplified also by the phase pictograms.

As indicated in Fig. 17, every basic mode has 7 subgroups, 3 of which (the interaction modes) are shared with the other three basic modes. This adds up to a total of 22 modes in the third level of the lattice. Six of them are interaction modes, and these are the ones that we are interested in. At this point it is good to note that **RT** is present in all four basic modes, and hence does nothing to discriminate between them. This means that we do not really need the **R** symmetry (which is

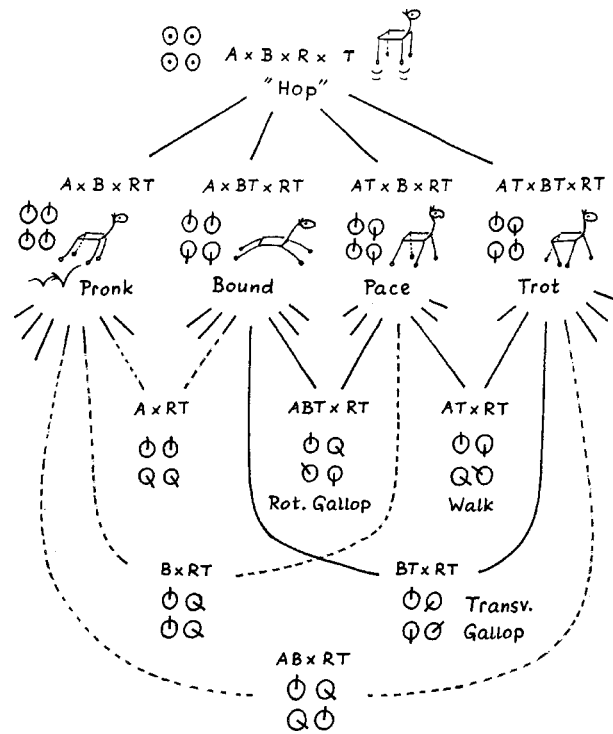


Fig. 17. The symmetry hierarchy of gaits corresponding to our four-pendulum model. The different gaits are shown by their group-theoretical structure, by their phase pictograms, and by a sketch of the animal (except at the level of the interaction gaits, where one sketch is not sufficient anymore to characterize a gait, cf. Fig. 18). The dashed lines indicate that the corresponding three interaction gaits are not observed in practice.

fortunate, since this symmetry is anything but perfect in real animals) and the basic modes may just as well be described by $\mathbf{A} \times \mathbf{B}$, $\mathbf{A} \times \mathbf{BT}$, $\mathbf{AT} \times \mathbf{B}$, and $\mathbf{AT} \times \mathbf{BT}$. This brings about a welcome economy in the daughter modes: There are precisely six of them (the interaction modes **A**, **B**, **AB**, **ABT**, **AT**, and **BT**, see also Ref. 28), and that is all.

The most important interaction mode is the walk ($\mathbf{AT} \times \mathbf{RT}$), the common daughter of the pace and the trot. In this gait, the feet are placed in the order 1342 1342 1342 etc. (see Fig. 14 for our numbering convention). Figure 18(a) shows a walking horse. Not any two legs are in phase anymore, but they are still pairwise in counter-phase. This is the primordial form of locomotion, presumably used by the first land animals (because of its stability: the center of mass is always within the triangle formed by the supporting legs) and is still the prevailing gait at low speed.¹⁹ The popularity of the walk may also have to do with the fact that it does not involve the **B** symmetry, which (as we know) is far from perfect in most animals. Crawling babies use this pattern too. So, whereas from a theoretical point of view the “hop” is the basic gait, from a practical and evolutionary standpoint the gait hierarchy starts with the walk.

Through the ages the animals have become faster, in an upward spiral of hunt and escape, and in the process have brought into practice almost all the gaits in the symmetry hierarchy.³¹ An accelerating horse will typically go from a walk to a trot and finally into a gallop. This sequence, which was beautifully corroborated in 1981 by the results of Hoyt and Taylor, in their landmark experiment with horses on a treadmill,²⁹ can also be recognized in the symmetry hierar-

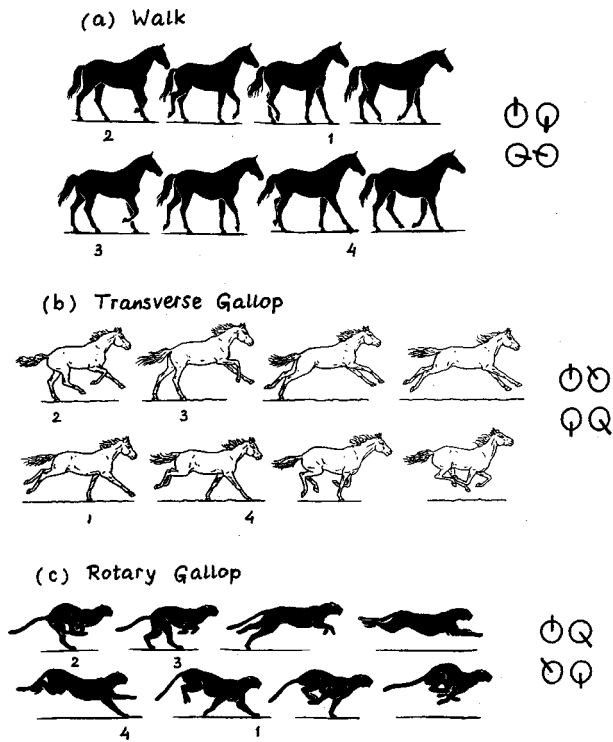


Fig. 18. (a) A walking horse, (b) a galloping horse (transverse gallop), and (c) a galloping cheetah (rotary gallop), all from Ref. 19. Eight stages are needed to fully characterize these gaits, whereas four were sufficient for the more symmetric gaits of Fig. 16. The numbers indicate in which order the legs are put on the ground. Walk: 1342. Transverse gallop: 1423. Rotary gallop: 1234.

chy of Fig. 17. The walking horse goes into a trot by means of a symmetry-restoring bifurcation, and from there into a (transverse) gallop. The transverse gallop is characterized by the pattern 1423 1423 1423 etc. It is illustrated in Fig. 18(b).

On the basis of the symmetry hierarchy it is even possible to speculate about the next evolutionary step. The horses of the future, in pursuit of still higher speeds, may go up one level again and learn to perform a bound (symmetry restoring bifurcation). They may also go down one level, toward a gait not depicted in Fig. 17 (symmetry breaking bifurcation). Or, since this is also possible at the level of the gallop, they may escape from the hierarchy by means of a Hopf bifurcation. This third option is particularly intriguing, since it would result in a gait with another periodicity (i.e., not $2T$), possibly even a quasiperiodic one.

In Fig. 19 we show a succession of gaits, based on our four-pendulum model, which contains all of the above ingredients. We have chosen a path through the (a, Ω) plane that passes reasonably close by the mode interaction points corresponding to the walk and the transverse gallop. Following this path, starting from the 0 motion or "hop," our pendulum animal first goes into a pace (in a rather abrupt way) and immediately afterwards switches to a walk. It duly exhibits the sequence

walk \rightarrow trot \rightarrow transverse gallop,

and becomes unstable before reaching the bound. Thus it seems, at least along this particular path, that apart from the physiological problems with the bound there is also a bifurcational impediment.

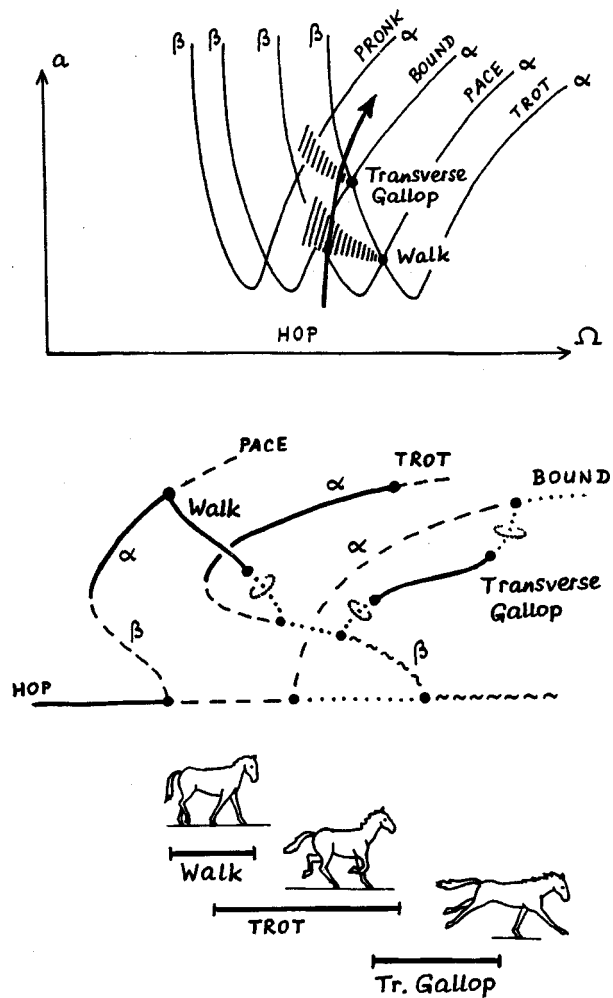


Fig. 19. Bifurcation diagram for our model quadruped, together with the associated path through the (a, Ω) plane. The succession of stable gaits contains the sequence walk-trot-gallop observed in real horses. Note the hysteresis at the various transitions (hop-pace, walk-trot, trot-gallop). For ease of survey, the 0 motion (hop) and the pure modes (direct branches from the 0 motion) have been denoted in capitals, and the interaction modes in lower-case letters.

Note that the bifurcations walk-trot and trot-gallop are hysteretic: When the animal is accelerating the (discontinuous) switch from trot to gallop occurs at a higher speed than the switch from gallop to trot when it slows down. This is precisely as in real horses.²⁹ It is also worth noting that the animal does not have to think about its steps; everything is determined by the particular arrangement of the four oscillators. The nervous system just has to intensify its signals [that is, to increase a in order to follow the proper path through the (a, Ω) plane] and the sequence comes about automatically.

Figure 19 depicts just one possible path through the (a, Ω) plane that contains the walk-trot-gallop sequence, and we do not claim that this one is better or more realistic than any other. But it does show the point we want to make, namely that the interaction (i.e., connection) between the modes is always established via common daughter modes in the symmetry hierarchy. In other words, the "general rule" found in the previous sections is also valid in the present context. It also shows, as noted before, that it is in the bifurcation dia-

gram with its bent curves and its cross branches (*not* in the symmetry lattice) that the nonlinear nature of the system becomes manifest.

One last remark: Apart from the walk and the transverse gallop, the only other interaction mode of practical importance is the rotary (or lateral) gallop. It derives its name from the fact that the feet are placed in the “rotational” order 1234 1234 1234 etc. Being the transition mode between the pace (a relatively slow gait) and the very swift bound, it is especially suited for those quadrupeds that want to accelerate in one stroke over a large speed interval. The cheetah [see Fig. 18(c)] is a prominent user of this type of gallop.¹⁹ The remaining three interaction modes in Fig. 17, which connect the pronk to the other pure modes, do not seem to be favored by any known animal (that is why the corresponding lines are dashed) and the current language has no names for them. A reason for this unpopularity may be that the pronk is a one-beat gait whereas the bound, pace and trot are two-beat gaits: apparently the two kinds do not mix very well.

V. CONCLUDING REMARKS

Let us briefly recapitulate the three main points. The first one is that mode interaction in a nonlinear system is quite a different affair than a simple superposition of two modes. The interaction modes exist in their own right, separated from their parents by a bifurcation, and with a lesser degree of symmetry. We have seen that mode interaction takes place not between just any two modes, but only between those that are linked in the symmetry hierarchy by a common daughter. This appears to be universally true and may well be called the quintessence of nonlinear mode interaction.

All the systems in the present paper were parametrically driven, and one might wonder if they are really representative (as far as the mode interaction is concerned) for systems of nonlinear oscillators in general. The answer seems to be yes. Of course, in this more general context, the symmetry hierarchy is not restricted to $2T$ -periodic oscillations interconnected by bifurcations that preserve the period.³² One also has to be prepared for types of bifurcation that alter the periodicity of the motions, and the hierarchy must be extended to encompass a multitude of periodicities. The motions with different periodicities can be accommodated in separate layers within the hierarchy, and these layers are interconnected (at certain points) via period doublings or Hopf bifurcations. This extended symmetry hierarchy is also known by its mathematical name as the “complete isotropy lattice.” Within this lattice, the interaction again takes place via common daughter modes, and that is how the general rule should be interpreted.

The second point is that the form, location, and stability of the interaction mode depend sensitively on the nonlinear terms in the system’s equations of motion. This explains why, in spite of the above unifying principle, the actual appearance of mode interaction can vary hugely from system to system, and even within one single system. For instance, any changes in the nonlinearity of the torsion spring in our two-pendulum model have a marked effect on the width of the interaction region and on the (order of) bifurcations inside this region.¹⁶ Another striking example is provided by the parametrically driven compound pendulum of Skeldon and Mullin,^{13,33} which has exactly the same $Z_2 \times Z_2 \times Z_2$ isotropy lattice as the two-pendulum system, but quite a different appearance in the (a, Ω) plane. Indeed, in cases where a gen-

eral understanding is not enough and information is required for a specific system, with specific values of the control parameters, one has to face the full equations of motion.

The third point is that mode interaction is all around us. Apart from the examples we have mentioned so far, mode interaction is found in the solidification of liquid crystals,³⁴ in the transverse “sloshing” waves in a canal,³⁵ in the tearing instabilities in a tokamak plasma,³⁶ in the chaotic signal of the pulsating star R Scuti,³⁷ and in many, many other systems. Indeed, as stated in the introduction, the world is full of coupled nonlinear oscillators and, hence, mode interaction.

ACKNOWLEDGMENTS

We are deeply indebted to Mark Kettenis, Jonathan Ross, Emile de Kleine, and Michel Oosterhof for their many contributions, their friendship, and their enthusiasm.

^aElectronic mail: j.p.vanderweele@tn.utwente.nl

¹J. Buck and E. Buck, “Synchronous fireflies,” *Sci. Am.* **234**, 74–85 (May 1976); see also W. Garver and F. Moss, “Electronic fireflies,” *ibid.* **251**, 94–96 (Dec 1993).

²A. Stefanovska, “Self-organisation of biological systems influenced by electric current,” thesis, University of Ljubljana, Slovenia, 1992.

³M. Faraday, “On a peculiar class of acoustical figures; and on certain forms assumed by groups of particles upon vibrating elastic surfaces,” followed by an “Appendix on the forms and states assumed by fluids in contact with vibrating elastic surfaces,” *Philos. Trans. R. Soc. London* **121**, 299–340 (1831).

⁴Alternatively, one may rhythmically alter the length of the pendulum. This way of parametric driving is found in the playground swing [the kind on which one has to squat (Ref. 5)] and in “O Botafumeiro,” the giant incense burner in Santiago de Compostella, Spain (Ref. 6).

⁵P. L. Tea Jr. and H. Falk, “Pumping on a swing,” *Am. J. Phys.* **36**, 1165–1166 (1968); A. E. Siegman, “Comments on pumping on a swing,” *ibid.* **37**, 843–844 (1969); J. A. Burns, “More on pumping on a swing,” *ibid.* **38**, 920–922 (1970); W. Case, “Parametric instability: An elementary demonstration and discussion,” *ibid.* **48**, 218–221 (1980).

⁶J. R. Sanmartín, “O Botafumeiro: Parametric pumping in the Middle Ages,” *Am. J. Phys.* **52**, 937–945 (1984).

⁷N. W. McLachlan, *Theory and Applications of Mathieu Functions* (Dover, New York, 1964).

⁸An excellent overview of the various forms of bifurcation that appear in the present paper can be found in S. H. Strogatz, *Nonlinear Dynamics and Chaos, with Applications in Physics, Biology, Chemistry, and Engineering* (Addison-Wesley, Reading, MA, 1994). See especially Chaps. 3 and 8. Another recommended introduction is R. C. Hilborn, *Chaos and Nonlinear Dynamics* (Oxford U.P., New York, 1994); see especially Sec. 3.18 on bifurcation theory.

⁹S. Ciliberto and J. P. Gollub, “Pattern competition leads to chaos,” *Phys. Rev. Lett.* **52**, 922–925 (1984); “Chaotic mode competition in parametrically forced surface waves,” *J. Fluid Mech.* **158**, 381–398 (1985).

¹⁰E. Meron and I. Procaccia, “Low-dimensional chaos in surface waves: Theoretical analysis of an experiment,” *Phys. Rev. A* **34**, 3221–3237 (1986); see also E. Meron and I. Procaccia, “Theory of chaos in surface waves: The reduction of hydrodynamics to few-dimensional dynamics,” *Phys. Rev. Lett.* **56**, 1323–1326 (1986); E. Meron, “Parametric excitation of multimode dissipative systems,” *Phys. Rev. A* **35**, 4892–4895 (1987).

¹¹M. Umeki and T. Kambe, “Nonlinear dynamics and chaos in parametrically excited surface waves,” *J. Phys. Soc. Jpn.* **58**, 140–154 (1989).

¹²J. D. Crawford, E. Knobloch, and H. Riecke, “Period-doubling mode interactions with circular symmetry,” *Physica D* **44**, 340–396 (1990); a short version of this paper can be found in the proceedings mentioned under Ref. 36.

¹³E. J. Banning, J. P. van der Weele, and M. M. Kettenis, “Mode competition in a system of two parametrically driven pendulums; the role of symmetry,” *Physica A* **247**, 281–311 (1997)

¹⁴E. J. Banning and J. P. van der Weele, “Mode competition in a system of two parametrically driven pendulums: The Hamiltonian case,” *Physica A* **220**, 485–533 (1995).

¹⁵E. J. Banning, J. P. van der Weele, J. C. Ross, M. M. Kettenis, and E. de

- Kleine, "Mode competition in a system of two parametrically driven pendulums: The dissipative case," *Physica A* **245**, 11–48 (1997).
- ¹⁶E. J. Banning, J. P. van der Weele, J. C. Ross, and M. M. Kettenis, "Mode competition in a system of two parametrically driven pendulums with nonlinear coupling," *Physica A* **245**, 49–98 (1997).
- ¹⁷In the case that the spring becomes very hard ($L > 0.2 K$) one even gets a third scenario, involving no fewer than two Hopf bifurcations, see Ref. 16.
- ¹⁸The Z stems from the German word for cyclic (*Zyklisch*). Another common notation for this group is C_2 . The reader who is not familiar with the groups appearing in the present paper may find a proper introduction in W. Ledermann, *Introduction to Group Theory* (Oliver and Boyd, Edinburgh, 1973). Most other texts on group theory will do as well. A particularly vivid and pedagogical introduction is Ref. 22.
- ¹⁹P. Gambaryan, *How Mammals Run: Anatomical Adaptations* (Wiley, New York, 1974), with beautiful illustrations.
- ²⁰D. Graham, "Pattern and control of walking in insects," *Adv. Insect Physiol.* **18**, 31–140 (1985).
- ²¹G. Schöner, W. Y. Yiang, and J. A. S. Kelso, "A synergetic theory of quadrupedal gaits and gait transitions," *J. Theor. Biol.* **142**, 359–391 (1990).
- ²²I. N. Stewart and M. Golubitsky, *Fearful Symmetry* (Penguin, London, 1992); animal gaits are discussed in Chap. 8.
- ²³J. J. Collins and I. N. Stewart, "Coupled nonlinear oscillators and the symmetries of animal gaits," *J. Nonlinear Sci.* **3**, 349–392 (1993).
- ²⁴J. J. Collins and I. N. Stewart, "Hexapodal gaits and coupled nonlinear oscillator models," *Biol. Cybern.* **68**, 287–298 (1993).
- ²⁵S. H. Strogatz and I. N. Stewart, "Coupled oscillators and biological synchronization," *Sci. Am.* **269**, 68–75 (1993).
- ²⁶H. Haken, *Principles of Brain Functioning: A Synergetic Approach to Brain Activity, Behavior and Cognition* (Springer, Berlin, 1996); animal gaits are discussed in Chap. 9.
- ²⁷G. Stamberg and D. Wilson, "Llamapaedia," <http://www.llamapaedia.com/anatomy/gaits.html>
- ²⁸J. P. van der Weele and E. J. Banning, "Mode interaction in a cup of coffee and other nonlinear oscillators," *J. Nonlinear Phenomena Complex Systems* **3**, 268–283 (2000).
- ²⁹D. F. Hoyt and C. R. Taylor, "Gaits and the energetics of locomotion in horses," *Nature (London)* **292**, 239–240 (1981).
- ³⁰Another man who was delighted with Muybridge's work was the artist Edgar Degas, whose fascination with horses and horse races took form in paintings, drawings, and even a series of horse sculptures. Many of these were based on pictures from the book "Animal Locomotion," published by Muybridge in 1887. Some seventeen sculptures still survive and are now in the Museum de Arte de São Paulo.
- ³¹In the meantime, also the walk itself has been brought to perfection, especially by the Paso Fino, the breed of horse that was brought to America by Columbus and used by the conquistadors on their long expeditions into the new world. Its "four beat lateral gait," a walk of great beauty, is said to be the smoothest ride in the world and has earned the Paso Fino its nickname, "the Rolls Royce of the Riding World."
- ³²In fact, even in the examples of the present paper, things were not so restricted as that, as remarked in Sec. III. The bifurcation from the 0 motion to the pure modes was actually a period doubling bifurcation.
- ³³A. C. Skeldon and T. Mullin, "Mode interaction in a double pendulum," *Phys. Lett. A* **166**, 224–229 (1992); A. C. Skeldon, "Dynamics of a parametrically excited double pendulum," *Physica D* **75**, 541–588 (1994).
- ³⁴H. Levine, W. J. Rappel, and H. Riecke, "Resonant interactions and traveling-solidification cells," *Phys. Rev. A* **43**, 1122–1125 (1991).
- ³⁵L. Shemer and S. Lichter, "The mode number dependence of neutral stability cross-waves," *Exp. Fluids* **9**, 148–152 (1990); W. B. Underhill, S. Lichter, and A. J. Bernoff, "Modulated, frequency-locked and chaotic cross-waves," *J. Fluid Mech.* **225**, 371–394 (1991).
- ³⁶R. Grauer, "Codimension two interactions of tearing modes," in *Proceedings of the International Conference on Singular Behavior and Nonlinear Dynamics, Samos, Greece, 1988*, edited by S. Pnevmatikos, T. Bountis, and S. Pnevmatikos (World Scientific, Singapore, 1989), Vol. 1, pp. 267–276.
- ³⁷J. R. Buchler, T. Serre, Z. Kollath and J. Mattei, "A chaotic pulsating star: The case of R Scuti," *Phys. Rev. Lett.* **73**, 842–845 (1995).